*J. Fluid Mech.* (1992), *vol.* 239, *pp.* 273–292
*Printed in Great Britain*



# Heteroclinic bifurcations in a simple model of double-diffusive convection

By E. KNOBLOCH[1], M. R. E. PROCTOR[2] AND N. O. WEISS[2]

[1] Department of Physics, University of California, Berkeley, CA 94720, USA

[2] Department of Applied Mathematics and Theoretical Physics, University of Cambridge, Silver Street, Cambridge CB3 9EW, UK

(Received 2 May 1991 and in revised form 19 November 1991)

Two-dimensional thermosolutal convection is perhaps the simplest example of an idealized fluid dynamical system that displays a rich variety of dynamical behaviour which is amenable to investigation by a combination of analytical and numerical techniques. The transition to chaos found in numerical experiments can be related to behaviour near a multiple bifurcation of codimension three. The resulting third-order normal form equations provide a rational approximation to the governing partial differential equations and thereby confirm that temporal chaos is present in thermosolutal convection. The complex dynamics is associated with a heteroclinic orbit in phase space linking a pair of saddle-foci with eigenvalues satisfying Shil'nikov's criterion. The same bifurcation structure occurs in a truncated fifth-order model and numerical experiments confirm that similar behaviour extends to a significant region of parameter space.

## 1. Introduction

In a fluid heated from below and stabilized by a composition gradient, rotation or a magnetic field, double-diffusive effects can lead to a rich variety of behaviour. Idealized thermosolutal convection has received considerable attention as the paradigm of a continuous fluid system where complicated dynamics arises from the competition between stabilizing and destabilizing mechanisms (Moore & Weiss 1990). In the regime of interest, where the ratio $\tau$ of the solutal to the thermal diffusivity is small, instability sets in at an oscillatory (Hopf) bifurcation; in a confined system this bifurcation leads to oscillations which take the form of standing waves and grow in amplitude as the thermal Rayleigh number is increased. Precise numerical experiments on two-dimensional convection in a container with aspect ratio of order unity show that these oscillations may eventually become chaotic before giving way to stable steady convection (Knobloch *et al.* 1986*b*; Moore, Weiss & Wilkins 1990*b*).

Similar behaviour is found in a truncated model in which the relevant partial differential equations are reduced to a set of five ordinary differential equations (Da Costa, Knobloch & Weiss 1981). In this system the origin of the chaos can be traced to a heteroclinic bifurcation. At this bifurcation there is an orbit in phase space that spirals in towards a pair of saddle-foci related by reflection symmetry. Behaviour then depends on the eigenvalues at these saddle-foci. Shil'nikov (1965) showed that a third-order system possessing a homoclinic orbit connecting a single saddle-focus, with eigenvalues $q$, $-p \pm i\omega$ ($q, p > 0$, $\omega \neq 0$), to itself contains in addi-

tion an uncountable number of non-stable non-periodic orbits whenever the ratio $\delta \equiv p/q < 1$. Consider now a system that depends on a control parameter $\lambda$ and suppose that the homoclinic orbit appears at $\lambda = \lambda_h$; at this parameter value there is then a homoclinic bifurcation in which a periodic orbit is destroyed. The complex sequence of bifurcations that produces infinitely many orbits as $\lambda \to \lambda_h$ was described by Glendinning & Sparrow (1984; see also Wiggins 1988). Essentially identical conclusions apply to heteroclinic orbits joining saddle-foci that are related by symmetry (Tresser 1984). In particular, if $\delta > 1$ then as $\lambda \to \lambda_h$ the period $P$ of a limit cycle tends to infinity monotonically and no chaos is present. For $\frac{1}{2} < \delta < 1$, $\lambda(P)$ oscillates about $\lambda_h$ as $P \to \infty$ and there may be intervals of stable chaos. If $\delta < \frac{1}{2}$ all orbits are unstable (though this case does not occur in a dissipative third-order system, for which $q-2p < 0$). These conclusions extend to higher dimensional systems provided the remaining eigenvalues $r_i$ satisfy $\mathrm{Re}\,(r_i) \ll -p$. In the regime where solutions of the fifth-order system are chaotic this condition is met and $\frac{1}{2} < \delta < 1$.

Comparison of solutions of the model system with those of the full partial differential equations suggests that the Shil'nikov mechanism is responsible for the presence of chaos in the latter system too. The chaos in the truncated model occurs, however, when that system no longer provides a rational approximation to the partial differential equations. Our aim here is to derive (in a certain limit) another set of ordinary differential equations which does not suffer from that disadvantage. This 'canonical' system is of third order and also exhibits chaos caused by the Shil'nikov mechanism. Thus we can show that the same process occurs in the partial differential equations governing thermosolutal convection.

A natural way of deriving low-order model systems is to focus on multiple bifurcation points in the parameter space and to obtain the normal forms for the dynamics near these points (Guckenheimer & Holmes 1986). Normal form equations provide a qualitatively accurate description of behaviour in a finite neighbourhood of a multiple bifurcation point. In this problem there are two bifurcations of codimension one, since the Hopf bifurcation is followed by a stationary bifurcation as the thermal Rayleigh number $R_T$ is increased. By varying both $R_T$ and the solutal Rayleigh number $R_S$ it is possible to locate the bifurcation of codimension two where the Hopf and pitchfork bifurcations coincide. Behaviour in the neighbourhood of this double bifurcation is described by second-order normal form equations (Knobloch & Proctor 1981; Coullet & Spiegel 1983). To include chaos we require a third-order system and so we need to introduce an additional parameter. We choose here to vary the aspect ratio $A$ and examine the multiple bifurcation when $A \to 0$. In the limit as $\tau \to 0$ the normal form equations reduce to the familiar Lorenz system (in a non-standard parameter range). Behaviour in the neighbourhood of the heteroclinic bifurcation is described by simpler equations (the canonical system) and there is a parameter range where the Shil'nikov mechanism leads to stable chaos.

We thus have an asymptotically exact system of ordinary differential equations that are derived rigorously (if a little artificially) from the governing partial differential equations. Standard hyperbolicity arguments now show that there exists a small but finite region of parameter space where the bifurcation structure associated with the Shil'nikov mechanism is preserved and stable chaos is present. We expect, moreover, that the multiple bifurcation will act as an organizing centre for behaviour in a significant region of parameter space and that the mechanism responsible for the presence of chaos will therefore be robust. This expectation is confirmed by numerical experiments.

In the next section we introduce the fifth-order system, first obtained by Veronis (1965), and show that it can be reduced to the third-order Lorenz system in the limit as $\tau \to 0$. These systems are only valid approximations to the original partial differential equations when the amplitudes of the solutions are small. The third-order system is investigated, for appropriate parameter values, in §3. There is a transition to chaos associated with a heteroclinic bifurcation at which Shil'nikov's condition is satisfied but this is typically in a regime where the third-order system is no longer a valid approximation to the partial differential equations. In §4 we show that in the limit $A \to 0$ the entire behaviour of the oscillatory branch can be accurately represented by third-order evolution equations. In particular, behaviour near the heteroclinic bifurcation is described by a particularly simple third-order system, hereafter referred to as the canonical system, which admits chaotic solutions; this system can also be derived directly as a rational approximation to the partial differential equations in this limit (Proctor & Weiss 1990). Finally, in §5, we relate different limiting procedures that lead to asymptotically valid evolution equations and compare our results with numerical experiments on thermosolutal convection and with other forms of double convection. Analogous results for magnetoconvection are summarized in the Appendix.

## 2. Truncated model systems

We consider two-dimensional Boussinesq convection with motion confined to the $(x, z)$-plane. Distances and times are measured in terms of the layer depth and the corresponding thermal diffusion time, respectively. Then the stream function $\Psi(x, z, t)$, the temperature fluctuation $\Theta(x, z, t)$ and the fluctuation in solute concentration $\Sigma(x, z, t)$ satisfy the non-dimensional equations

$$\partial_t \nabla^2 \Psi + \partial(\Psi, \nabla^2 \Psi) = \sigma[R_T \partial_x \Theta - R_S \partial_x \Sigma + \nabla^4 \Psi], \tag{1a}$$

$$\partial_t \Theta + \partial(\Psi, \Theta) = \partial_x \Psi + \nabla^2 \Theta, \tag{1b}$$

$$\partial_t \Sigma + \partial(\Psi, \Sigma) = \partial_x \Psi + \tau \nabla^2 \Sigma \tag{1c}$$

in the region $\{0 \leqslant x \leqslant A; 0 < z < 1\}$, where $\sigma$ is the ratio of the viscous to the thermal diffusivity (e.g. Knobloch *et al.* 1986*b*). For convenience we adopt the idealized boundary conditions

$$\Psi = \partial_z^2 \Psi = \Theta = \Sigma = 0 \qquad \text{on} \quad z = 0, 1, \tag{2a}$$

$$\Psi = \partial_x^2 \Psi = \partial_x \Theta = \partial_x \Sigma = 0 \quad \text{on} \quad x = 0, A. \tag{2b}$$

The system (1)–(2) then possesses the point symmetry

$$(x, z) \to (A - x, 1 - z), \quad (\Psi, \Theta, \Sigma) \to (\Psi, -\Theta, -\Sigma). \tag{3}$$

We assume that $A$ is sufficiently small that the trivial solution $\Psi = \Theta = \Sigma = 0$ first becomes unstable to modes with a single roll in the box. In the neighbourhood of such a bifurcation we set

$$\Psi = 2[2(1 + A^2)]^{\frac{1}{2}} a(t^*) \sin(\pi x / A) \sin \pi z + O(a^3), \tag{4a}$$

$$\Theta = \frac{2A}{\pi}\left[\frac{2}{1 + A^2}\right]^{\frac{1}{2}} b(t^*) \cos\left(\frac{\pi x}{A}\right) \sin \pi z - \frac{1}{\pi} c(t^*) \sin 2\pi z + O(a^3), \tag{4b}$$

$$\Sigma = \frac{2A}{\pi}\left[\frac{2}{1 + A^2}\right]^{\frac{1}{2}} d(t^*) \cos\left(\frac{\pi x}{A}\right) \sin \pi z - \frac{1}{\pi} e(t^*) \sin 2\pi z + O(a^3), \tag{4c}$$

where the modified time $t^* = [\pi^2(1+A^2)/A^2]t$. These expressions contain all terms that appear to first and second order in a modified perturbation expansion and also possess the point symmetry (3). Substituting from (4) into (1) we obtain the fifth-order system

$$\dot{a} = \sigma[-a + r_T b - r_S d] + O(a^5), \tag{5a}$$

$$\dot{b} = -b + a(1-c) + O(a^5), \tag{5b}$$

$$\dot{c} = \varpi(-c + ab) + O(a^4), \tag{5c}$$

$$\dot{d} = -\tau d + a(1-e) + O(a^5\tau^{-4}), \tag{5d}$$

$$\dot{e} = \varpi(-\tau e + ad) + O(a^4\tau^{-3}), \tag{5e}$$

where dots indicate differentiation with respect to $t^*$ (Veronis 1965; Da Costa *et al.* 1981). Here the scaled Rayleigh numbers

$$r_T = R_T/R_0, \quad r_S = R_S/R_0, \quad R_0 = \pi^4(1+A^2)^3/A^4, \tag{6}$$

while the geometrical factor

$$\varpi = 4A^2/(1+A^2) \quad (0 < \varpi < 4). \tag{7}$$

The fifth-order system obtained by neglecting terms $O(a^4)$ in (5) becomes exact in the limit $|a| \to 0$ (small Péclet number); for small to moderate $|a|$ it still provides a qualitatively correct description of the dynamics of the full partial differential equations (Knobloch *et al.* 1986*b*).

This fifth-order system can be simplified by proceeding to the limit $\tau \to 0$ (for a salt–water mixture at room temperature $\tau = 0.012$). Let $\tilde{t} = \tau t^*$ be a slow time and set

$$r_T = 1 + \tau r, \quad r_S = \tau^2 s, \quad a = \tau\tilde{a}, \quad b = \tau\tilde{b}, \quad c = \tau^2\tilde{c}, \tag{8}$$

where the quantities with tildes are taken to be of order unity. Then from (5*b*) we obtain

$$\tilde{b} = \tilde{a} - \tau\tilde{a}' + O(\tau^2), \tag{9}$$

where the prime denotes differentiation with respect to $\tilde{t}$. Equation (5*c*) decouples, leaving the third-order system

$$\tilde{a}' = (1+\lambda)\,\tilde{a} - (1+\mu)\,d + O(\tau\tilde{a}), \tag{10a}$$

$$d' = -d + \tilde{a}(1-e) + O(\tilde{a}^5), \tag{10b}$$

$$e' = \varpi(-e + \tilde{a}d) + O(\tilde{a}^4), \tag{10c}$$

where

$$r = \sigma^{-1}(1+\sigma)\,(1+\lambda), \quad s = \sigma^{-1}(1+\sigma)\,(1+\mu). \tag{11}$$

In this limit the temperature is only slightly perturbed by the motion but the perturbations to the solute concentration are of order unity. Once again, we may only neglect the higher-order terms in (10*b*) and (10*c*) if $|\tilde{a}| \ll 1$ and the solutal Péclet number is small. In the limit $\tau \to 0$ and $|\tilde{a}| \to 0$ we have, after suppressing tildes, the system

$$a' = (1+\lambda)\,a - (1+\mu)\,d, \tag{12a}$$

$$d' = -d + a(1-e), \tag{12b}$$

$$e' = \varpi(-e + ad). \tag{12c}$$

This system possesses the symmetry $(a, d, e) \to (-a, -d, e)$ and is dissipative if and only if $\lambda < \varpi$.

From (12*a*) and (12*b*) it follows that

$$a''-\lambda a'+(\mu-\lambda)a=(1+\mu)ae. \tag{13}$$

Thus there is a pitchfork bifurcation from the trivial solution at $\lambda=\mu$ and a Hopf bifurcation at $\lambda=0$ for $\mu>0$, with a multiple bifurcation at $\lambda=\mu=0$. It can be shown that the Hopf bifurcation is always supercritical and that there is a non-trivial steady solution in the neighbourhood of the pitchfork bifurcation which exists only for $\lambda<\mu$ and is always unstable. These results are valid for the full system (1)–(2) in the limit $\tau\to 0$.

The third-order system (12) has a steady solution with

$$a^2=a_0^2\equiv(\mu-\lambda)/(1+\lambda)\quad(-1<\lambda\leqslant\mu). \tag{14}$$

Thus $|a|$ increases monotonically with decreasing $\lambda$ along the branch of steady solutions, which is asymptotic to the line $\lambda=-1$. From (6), (8) and (11) this line corresponds to $r_T=1$ or $R_T=R_0$, the value at which convection sets in when $R_S=0$. It is well-known that steady convection can occur arbitrarily close to $R_T=R_0$ when $\tau\ll 1$ (Proctor 1981). Indeed, a higher-order approximation shows that there is a turning point on the steady branch which acquires stability in a saddle-node bifurcation for $a^2=O[(s/\tau)^{\frac{1}{2}}]$. These stable steady solutions, which exist both for the partial differential equations and for the fifth-order system, lie outside the range of our approximations.

Equations (12) can be cast into a more familiar form. Under the rescaling $x=\varpi^{\frac{1}{2}}a$, $y=\tilde{r}\varpi^{\frac{1}{2}}d$, $z=\tilde{r}e$, with $\tilde{r}=s/r=(1+\mu)/(1+\lambda)$ and $\tilde{\sigma}=-(1+\lambda)$ they are transformed into the Lorenz (1963) equations

$$x'=\tilde{\sigma}(y-x),\quad y'=\tilde{r}x-y-xz,\quad z'=-\varpi z+xy. \tag{15}$$

Most studies of this system have focused on transitions to chaos as $\tilde{r}$ is increased for some fixed $\tilde{\sigma}>0$ (Sparrow 1982). In our problem $\tilde{\sigma}<0$; this case is also relevant to laser physics and Elgin & Molina Garza (1988) have explored behaviour as $\tilde{\sigma}$ is decreased for fixed $\tilde{r}$. Here we are interested in codimension-one bifurcations that appear as $\lambda$ is varied for fixed $\mu$ (i.e. in varying $r_T$ for fixed $r_S$).

Equations (12) or (13) may be written in yet another form by defining

$$c=(1+\mu)e+\tfrac{1}{2}\varpi a^2. \tag{16}$$

Then we can eliminate $d$ to obtain

$$a''-\lambda a'+(\mu-\lambda)a=ac-\tfrac{1}{2}\varpi a^3, \tag{17a}$$

$$c'=\varpi[-c+Ka^2], \tag{17b}$$

where $K=\frac{1}{2}\varpi+(1+\lambda)$. Furthermore, by introducing a time-dependent potential $V(a,f)=\frac{1}{2}fa^2+\frac{1}{8}\varpi a^4$ (cf. Marzec & Spiegel 1980) we can rewrite (17) in the form

$$a''-\lambda a'=-\partial V/\partial a,\quad f'=-\varpi[f+K(a^2-a_1^2)] \tag{18}$$

with $a_1^2=(\mu-\lambda)/K$.

## 3. Heteroclinicity and chaos

In this section we shall investigate the Lorenz system (12) in the parameter range where $0<\varpi<4$ and $\mu>0$. First of all we establish that the branch of oscillatory solutions terminates in a heteroclinic bifurcation. For $\mu$ sufficiently small the

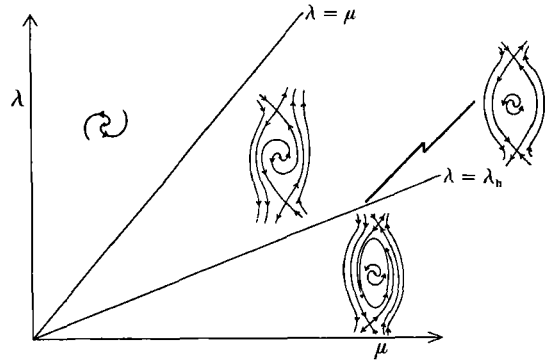


FIGURE 1. Unfolding diagrams for equation (20) in the neighbourhood of the multiple bifurcation point at $\lambda = \mu = 0$, showing the lines of Hopf bifurcations ($\lambda = 0$), homoclinic bifurcations ($\lambda = \lambda_h$) and pitchfork bifurcations ($\lambda = \mu$), together with relevant phase portraits.

heteroclinic orbit links two saddles, corresponding to unstable steady solutions with real eigenvalues. As $\mu$ increases, two of these eigenvalues merge to form a complex-conjugate pair, with negative real part, so that the heteroclinic orbit spirals into a symmetrical pair of saddle-foci. When $\mu$ is sufficiently large the eigenvalues at the saddle-foci satisfy Shil'nikov's condition and numerical solutions provide examples of complicated dynamics, including period-doubling and chaos. In describing these results we need to distinguish carefully between features that appear when the third-order system is a valid approximation to the partial differential equations and other properties peculiar to the Lorenz system (which is interesting in its own right).

The third-order system provides a correct description of the dynamics near the codimension-two bifurcation at the origin in the $(\lambda, \mu)$-plane. If we introduce a small parameter $\epsilon$ ($0 < \epsilon \ll 1$), together with the rescaling

$$\lambda = \epsilon^2\tilde{\lambda}, \quad \mu = \epsilon^2\tilde{\mu}, \quad a = \epsilon\tilde{a}, \quad c = \epsilon^2\tilde{c}, \quad \tilde{t} = \epsilon t \tag{19}$$

and immediately suppress the tildes then (17) simplifies to the normal form equation

$$a'' + (\mu - \lambda)a - a^3 = \epsilon\left(\lambda - \frac{2+\varpi}{\varpi}a^2\right)a' + O(\epsilon^2) \tag{20}$$

for a Bogdanov bifurcation with $Z_2$ symmetry (Knobloch & Proctor 1981; Coullet & Spiegel 1983). The oscillatory branch terminates in a heteroclinic orbit at $\lambda = \lambda_h$ (where the eigenvalues on the steady branch are real) with

$$a' \approx \pm(2a_h)^{-\frac{1}{2}}(a_h^2 - a^2), \quad a \approx \pm a_h \tanh\left[(\tfrac{1}{2}a_h)^{\frac{1}{2}}t\right], \tag{21}$$

where $a_h^2 = \mu - \lambda_h$. Moreover, we can combine (21) with the relation

$$\oint\left[\lambda - \frac{2+\varpi}{\varpi}a^2\right]a'^2\,\mathrm{d}t = O(\epsilon), \tag{22}$$

where the integral is taken round any periodic orbit of (20), to obtain the line

$$\lambda_h = \frac{2+\varpi}{2(1+3\varpi)}\mu + O(\epsilon), \tag{23}$$

on which the heteroclinic bifurcations occur. Figure 1 shows the locations of local and global bifurcations in the $(\lambda, \mu)$-plane together with the resulting phase portraits. The

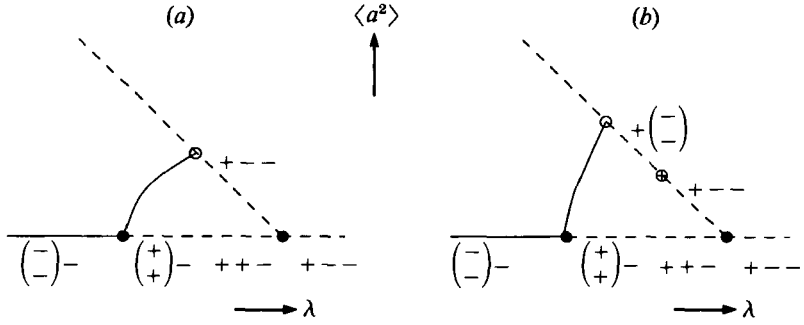


FIGURE 2. Bifurcation diagrams for equation (17). Sketches showing the mean-square amplitude $\langle a^2 \rangle$ as a function of $\lambda$ along branches of steady and periodic solutions. The signs of the real parts of eigenvalues are indicated along the steady branches. (Parentheses denote complex pairs.) (*a*) Real eigenvalues for non-trivial steady solutions, with the heteroclinic orbit connecting a pair of saddlepoints, as for equation (20); (*b*) complex eigenvalues,with a heteroclinic connection between a pair of saddle-foci.

corresponding bifurcation diagram, showing codimension-one behaviour as $\lambda$ is increased for fixed $\mu > 0$, is sketched in figure 2(*a*); the signs of the real parts of the relevant eigenvalues are indicated in the figure.

Further away from the codimension-two point the problem is described by (17) and chaotic dynamics may occur. The key to its development is provided by the eigenvalues $\rho$ along the branch of unstable steady solutions. These are given by the cubic equation

$$\rho^3+\rho^2[\varpi-\lambda]-\rho\varpi\left[1+\lambda-\frac{1+\mu}{1+\lambda}\right]-2\varpi(\mu-\lambda)=0; \tag{24}$$

near $\lambda = \mu$ they are real with one eigenvalue positive. Further along the steady branch the two negative eigenvalues become equal along the line E, shown in figure 3 for $\varpi = \frac{8}{3}$, and thereafter form a complex-conjugate pair. If the heteroclinic orbit forms in this region it will have a fully three-dimensional structure and the appearance of chaos becomes possible. If the eigenvalues are

$$\rho = q,\ -p \pm \mathrm{i}\omega\ (p, q > 0)$$

then behaviour depends on the ratio

$$\delta = p/q, \tag{25}$$

evaluated when the heteroclinic orbit forms. Stable chaos occurs in the neighbourhood of the global bifurcation for values of $\delta$ within the range $\frac{1}{2} < \delta < 1$ (Glendinning & Sparrow 1984; Wiggins 1988). The line $\delta = 1$ is given by

$$2(\varpi-\lambda)^3-\varpi(\varpi-\lambda)\left[1+\lambda-\frac{1+\mu}{1+\lambda}\right]-2\varpi(\mu-\lambda)=0, \tag{26}$$

while $\delta = \frac{1}{2}$ on $\lambda = \varpi$. These lines are also shown in figure 3 for $\varpi = \frac{8}{3}$. The heteroclinic bifurcations lie on the line $\lambda = \lambda_h$ whose slope near the origin is given by (23); for $\mu = O(1)$ its position has to be found numerically. We have computed its approximate position for $\varpi = \frac{8}{3}$ ($A = \sqrt{2}$), which is also shown in figure 3. The line starts in region I, with real eigenvalues, and then crosses into region II, where there are complex eigenvalues with $\delta > 1$. Stable chaotic behaviour is expected in the neighbourhood of the point, at $\mu \approx 4.62$, where the line enters region III, with $\frac{1}{2} < \delta < 1$. Finally, for

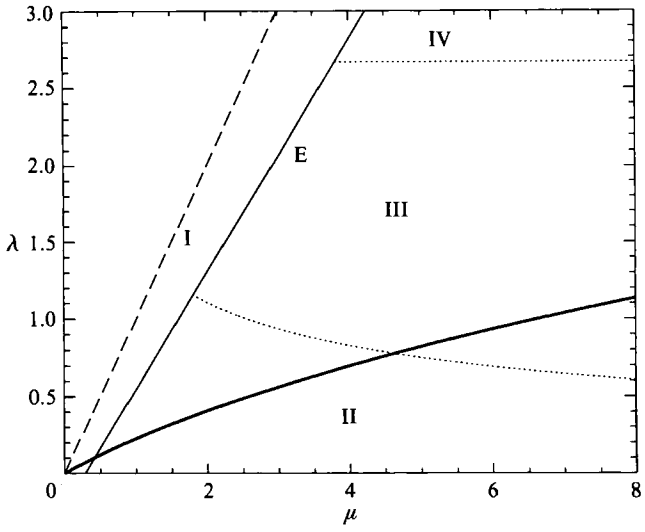


FIGURE 3. Heteroclinic bifurcations in the $(\mu, \lambda)$-plane for the Lorenz system (17) with $\varpi = \frac{8}{3}$. Non-trivial steady solutions exist to the right of the dashed line. In region I eigenvalues are real; in region II $\delta > 1$, in region III $\frac{1}{2} < \delta < 1$ and in region IV $0 < \delta < \frac{1}{2}$. The heavy line indicates the computed positions of the heteroclinic bifurcation: stable chaos is expected when it lies in region III.

$\mu$ sufficiently large, the line crosses into region IV with $0 < \delta < \frac{1}{2}$, where no attractors can exist. The bifurcation diagram corresponding to a value of $\mu$ such that the heteroclinic bifurcation lies in region III is sketched in figure 2(*b*). Note that there is now a transition from real to complex eigenvalues along the unstable steady branch.

Numerical integration of the equations provides examples of symmetry-breaking, period-doubling and chaotic behaviour consistent with the Shil'nikov mechanism (cf. Proctor & Weiss 1990). For example, with $\mu = 5.5$ there is a transition from a symmetric (S1) orbit to an asymmetric (P1) orbit at $\lambda \approx 0.7$, followed by successive period-doubling bifurcations that accumulate and are followed by an interval of chaos around $\lambda \approx 0.83$, where $\delta \approx 0.94$. In this parameter range the solutions have an amplitude $a_0 \approx 1.6$, so the Lorenz system is no longer a valid approximation to the original fluid dynamical problem. Similar behaviour has been found numerically for different choices of the parameter $\varpi$ in the range $0.01 \leqslant \varpi \leqslant 4$. Moreover, trajectories spiralling in towards saddle-foci have been illustrated by Elgin & Molina Garza (1988) for the case $\lambda \approx 2.3$, $\mu \approx 52$, $\varpi = 0.5$ (see also Weiss 1987). Thus there can be no doubt that the Shil'nikov mechanism leads to chaos in the system (12) with $\mu > 0$.

The amplitude of the chaotic oscillations decreases with decreasing $\varpi$. For $\varpi = 0.01$ and $\mu = 0.002$ the heteroclinic bifurcation occurs around $\lambda = 0.0019$ with $\delta \approx 0.88$ and the oscillations have an amplitude $a_0 \approx 0.01$. In this parameter range, where $|a| \ll 1$, we therefore expect the model system to be an accurate approximation to the partial differential equations. These numerical results suggest that we should explore behaviour for $\varpi \ll 1$ in greater detail in order to demonstrate that the same mechanism leads to chaotic oscillations in the full partial differential equations.

## 4. Tall thin cells

To proceed further analytically we need to capture more behaviour in the low-amplitude regime than is covered by the second-order normal form (20). Specifically, we want to bring the transition from real to complex eigenvalues along the steady branch into a range where $|a^2| \ll 1$. This can be achieved by adjusting the parameters so as to approach the codimension-three bifurcation at $\lambda = \mu = \varpi = 0$. Thus we proceed to the limit $\varpi \to 0$. Then the interesting dynamics occurs in a regime where $|a| = O(\varpi^{\frac{1}{2}}) \ll 1$ and the third-order system is indeed a valid approximation to the original partial differential equations. It turns out, however, that different orderings are appropriate at the beginning and end of the oscillatory branch, so these regimes have to be considered separately and then matched together.

### 4.1. *Nonlinear oscillations*

For $0 < \mu \ll \varpi \ll 1$ we recover a simplified normal form equation for the Bogdanov bifurcation. From (23), $\lambda_h \approx \mu(1-\frac{5}{2}\varpi)$: thus the heteroclinic bifurcation is close to the pitchfork bifurcation in this limit. In order to find more interesting behaviour we take $\mu = O(\varpi)$ and introduce the scaling

$$\lambda = \varpi\tilde{\lambda}, \quad \mu = \varpi\tilde{\mu}, \quad a = \varpi^{\frac{1}{2}}\tilde{a}, \quad c = \varpi c, \quad \tilde{t} = \varpi^{\frac{1}{2}}t. \tag{27}$$

Then, suppressing tildes as usual, we obtain from (17) the equations

$$a'' + (\mu-\lambda)\,a - ac = \varpi^{\frac{1}{2}}\lambda a' + O(\varpi), \tag{28a}$$

$$c' = \varpi^{\frac{1}{2}}(-c+a^2) + O(\varpi^{\frac{3}{2}}). \tag{28b}$$

At leading order we have $c = C =$ constant from (28*b*) and

$$a = A\sin\Omega t, \quad a' = \Omega A\cos\Omega t, \quad Q \equiv \Omega^2 = \mu-\lambda-C \tag{29}$$

from (28*a*). Moreover there is a conserved energy

$$E \equiv a'^2 + \Omega^2 a^2 = \Omega^2 A^2. \tag{30}$$

Both $E$ and $Q$ evolve on the slower timescale $T = \varpi^{\frac{1}{2}}t$ according to

$$E_T = 2\lambda a'^2 + a^2 c - a^4, \quad Q_T = c - a^2. \tag{31}$$

Averaging the right-hand sides we therefore obtain

$$E_T = \lambda\Omega^2 A^2 + \tfrac{1}{2}CA^2 - \tfrac{3}{8}A^4 = (\lambda-\tfrac{1}{2})E + (\mu-\lambda)\frac{E}{2Q} - \frac{3E^2}{8Q^2}, \tag{32a}$$

$$Q_T = (\mu-\lambda) - Q - \tfrac{1}{2}A^2 = (\mu-\lambda) - Q - \frac{E}{2Q}. \tag{32b}$$

The fixed points of this reduced system give the periodic orbits of (28), with

$$Q = \Omega^2 = \frac{\mu-\lambda}{4\lambda+1}, \quad A^2 = \frac{E}{Q} = \frac{8\lambda(\mu-\lambda)}{4\lambda+1}. \tag{33}$$

Thus the period, $P = 2\pi/\Omega$, of the oscillation increases monotonically from the Hopf bifurcation at $\lambda = 0$ to the end of the oscillatory branch, in the neighbourhood of the pitchfork bifurcation at $\lambda = \mu$. The amplitude $A$ rises to a maximum $A_c$ at $\lambda = \lambda_c$, where

$$\lambda_c = \tfrac{1}{4}[(1+4\mu)^{\frac{1}{2}} - 1], \quad A_c^2 = 2\mu + 1 - (1+4\mu)^{\frac{1}{2}}, \tag{34}$$

and then drops down towards zero as $\lambda$ approaches $\mu$. Along the unstable steady branch $a^2 = a_0^2 = \mu - \lambda$ and $A^2 > a_0^2$ at $\lambda = \lambda_c$ if $\mu > \frac{3}{4}$. Note that the oscillatory solution (29) is described by (33) along almost the entire length of the oscillatory branch. It is only in the neighbourhood of the heteroclinic bifurcation, when $0 < \mu - \lambda = O(\varpi)$, that $P \to \infty$ and the ordering (27) breaks down.

### 4.2. *The heteroclinic bifurcation*

To describe behaviour near the end of the oscillatory branch we adopt the scaling

$$\mu = \varpi\tilde{\mu}, \quad \lambda = \varpi\tilde{\lambda} = \varpi(\tilde{\mu} - \varpi\nu), \quad a = \varpi\hat{a}, \quad c = \varpi^2\hat{c}, \quad \hat{t} = \varpi t \tag{35}$$

instead of (27). Then, dropping hats and tildes, we find that (17) reduces to the system

$$a'' - \mu a' + \nu a = ac + O(\varpi), \tag{36a}$$

$$c' = -c + a^2 + O(\varpi). \tag{36b}$$

This canonical system can also be derived directly as a rational approximation to the partial differential equations (1) in the limit $A \to 0$, $\tau \to 0$ (Proctor & Weiss 1990).

The Hopf bifurcation in (17) lies outside the range of the scaling (35) but we can establish that equations (36) possess oscillatory solutions which, in the limit $\nu \to \infty$, match those given by (29) and (33). In this limit we introduce a small parameter $\epsilon = \nu^{-\frac{1}{2}}$ and let

$$a = \nu^{\frac{1}{2}}\bar{a}, \quad c = \nu\bar{c}, \quad \bar{t} = \nu^{\frac{1}{2}}t. \tag{37}$$

Then (36) becomes, after bars have been dropped,

$$\ddot{a} + a(1-c) = \epsilon\mu\dot{a}, \tag{38a}$$

$$\dot{c} = \epsilon(a^2 - c), \tag{38b}$$

where dots indicate differentiation with respect to $\bar{t}$. At leading order $c = C$, where both $C$ and $E \equiv \dot{a}^2 + a^2(1-c)$ vary slowly, and we obtain the following averaged equations:

$$E' = 2\mu\langle\dot{a}^2\rangle - \langle a^4\rangle + C\langle a^2\rangle, \quad C' = \langle a^2\rangle - C. \tag{39}$$

Thus we take

$$a = A\sin\Omega t, \quad \dot{a} = A\Omega\cos\Omega t, \quad Q \equiv \Omega^2 = 1 - C, \tag{40}$$

whence

$$E' = \mu E - \frac{3E^2}{8Q^2} + (1-Q)\frac{E}{2Q}, \quad Q' = 1 - Q - \frac{E}{2Q}. \tag{41}$$

The fixed points of (41) give periodic orbits of (38) with

$$Q = \Omega^2 = \frac{1}{4\mu + 1}, \quad A^2 = \frac{8\mu}{4\mu + 1}. \tag{42}$$

We can now check that (42) is consistent with (33), after taking the different scalings into account. Rewriting (42) in terms of the original variables in (17) we obtain

$$\Omega^2 = \frac{\varpi(\mu - \lambda)}{4\mu + \varpi}, \quad A^2 = \frac{8\mu(\mu - \lambda)}{4\mu + \varpi}, \tag{43}$$

in agreement with (33) in the limit $\lambda \to \mu$. So we have confirmed that the inner and outer limits in the two regions match for $\varpi \ll 1$. This matching is illustrated in figure 4(*a*) for $\varpi = 0.01$, $\tilde{\mu} = \mu/\varpi = 0.2$. Here the period $P = 2\pi/\Omega$ is plotted against

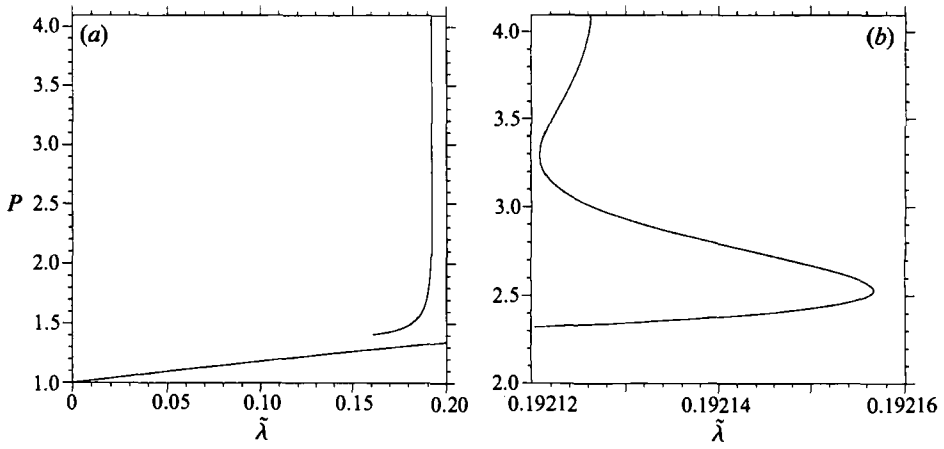


FIGURE 4. The approach to heteroclinicity when $\varpi \ll 1$. (*a*) The period $P$ as a function of $\tilde{\lambda}$ for $\varpi = 0.01$, $\tilde{\mu} = 0.2$. The lower curve shows the period computed from (33), while the upper curve is computed from (43). The mismatch diminishes as $\varpi \to 0$. (*b*) Enlargement showing the wiggly approach to heteroclinicity at $\tilde{\lambda} \approx 0.192$.

$\tilde{\lambda} = \lambda/\varpi$. The curve emerging from the Hopf bifurcation at $\tilde{\lambda} = 0$ is given by (33). The mismatch between the two curves is $O(\varpi^{\frac{1}{2}})$, as expected from the theory. The approach to heteroclinicity is magnified in figure 4(*b*), which shows the characteristic oscillations in $P(\tilde{\lambda})$ associated with the Shil'nikov mechanism. Thus we expect to find chaotic behaviour in this narrow region.

### 4.3. *Chaotic oscillations*

Theoretical analysis of the behaviour associated with a heteroclinic connection between a symmetrical pair of saddle-foci relies on reducing the flow described by ordinary differential equations to a one-dimensional map (Glendinning & Sparrow 1984; Wiggins 1988). The approach to heteroclinicity depends on the eigenvalues at the saddle-foci. From the one-dimensional map we can predict that if there is a continuous transition from $\delta > 1$ to $\delta < 1$ at the heteroclinic bifurcation then there exists a finite parameter range where stable chaos is present. As $\delta$ is reduced in the range $1 > \delta > \frac{1}{2}$ subsidiary homoclinic and heteroclinic orbits form, producing gaps in which no stable solutions can be found. In order to demonstrate the presence of chaos caused by the Shil'nikov mechanism it is therefore necessary to calculate the value of $\delta$ at the heteroclinic bifurcation and to show that it passes through unity. How far stable chaos persists into the range where $1 > \delta > \frac{1}{2}$ depends on non-local behaviour which cannot readily be predicted.

The system (36) has been discussed by Proctor & Weiss (1990). They found that the eigenvalues at the heteroclinic bifurcation varied continuously and that there was a transition from $\delta > 1$ to $\delta < 1$ at $\mu = 0.15$, with Shil'nikov's criterion satisfied for $\mu > 0.15$. They also confirmed numerically that stable chaotic solutions existed in the neighbourhood of this bifurcation. Now equations (36) are a valid approximation to the partial differential equations (1) in the limit $\tau \downarrow 0$, $\varpi \downarrow 0$ if

$$1 < \frac{\sigma r_S}{\tau^2(1+\sigma)} = 1 + O(\varpi) \tag{44a}$$

and

$$0 < \frac{\sigma[r_S - \tau(r_T - 1)]}{\tau^2(1+\sigma)} = O(\varpi^2), \tag{44b}$$

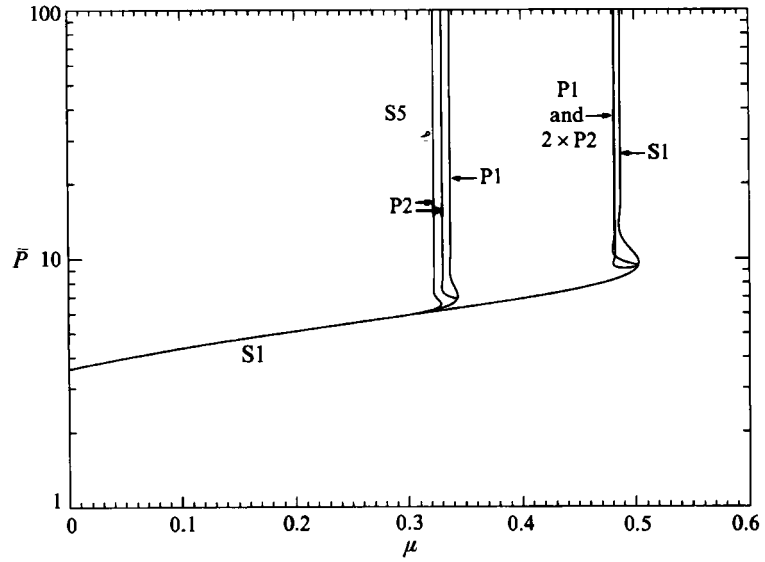


FIGURE 5. Heteroclinic and homoclinic orbits for the canonical system (36) with $\nu = 3.08$. The curves show the normalized period $\bar{P}$ as a function of $\mu$ along the S1 branch, with a heteroclinic bifurcation at $\mu = 0.487$, together with two P1 branches approaching homoclinicity at $\mu = 0.337$, 0.482, and four branches of P2 solutions. The tiny window with S5 solutions, located by Proctor & Weiss (1990) in the middle of a chaotic region, is also indicated, but with the period $P = 5\bar{P}$ to avoid confusion.

i.e. $s-r = O(\varpi^2)$, cf. (11). All of the complicated dynamics associated with the Shil'nikov mechanism is found within this narrowly restricted parameter range. Thus chaos can occur arbitrarily close to the onset of convection.

The third-order system (36) provides a canonical description of chaotic behaviour associated with a heteroclinic bifurcation at which Shil'nikov's criterion is satisfied, and is therefore worth studying in its own right. Numerical integration of these canonical equations provides examples of period-doubling cascades, followed by chaos interspersed with periodic windows (Proctor & Weiss 1990). It is convenient to investigate behaviour by increasing $\mu$ for fixed $\nu$ in (36); this corresponds to increasing $\mu$ while keeping $(\mu-\lambda)$ constant in (17). Then the Hopf bifurcation at $\mu = 0$ gives rise to a symmetric (S1) orbit of period $P$ such that

$$a(t+\tfrac{1}{2}P) = -a(t), \quad c(t+\tfrac{1}{2}P) = c(t). \tag{45}$$

Figure 5 shows $P$ as a function of $\mu$ along this branch for $\nu = 3.08$. As expected, the period increases as the branch wiggles towards a heteroclinic bifurcation at $\mu = 0.487$, where $\delta = 0.646$.

Chaotic behaviour appears within bubbles on alternate wiggles of the S1 curve (Glendinning & Sparrow 1984; Wiggins 1988) and the first bubble is usually most prominent. For small $\nu$ the bubble only contains a pair of secondary bifurcations at which the symmetry (45) is broken, giving rise to branches of asymmetric (P1) oscillations. As $\nu$ is increased twin cascades of period-doubling and period-halving bifurcations appear and eventually lead to chaos (Knobloch & Weiss 1983). Within the chaotic region are windows where periodic solutions appear at saddle-node bifurcations and undergo their own cascades of bifurcations. As $\nu$ is further increased the bubble opens owing to the formation of subsidiary homoclinic and heteroclinic orbits (Bernoff 1986). The behaviour of period-$n$ solutions can be represented by plotting their mean period $\bar{P} = P/n$. Figure 5 shows twin branches of P1 solutions

which themselves wiggle towards homoclinicity, as well as corresponding branches for period-doubled (P2) orbits, together with symmetric period-five (S5) solutions which appear within a tiny window (cf. Bernoff 1986; Weiss 1987; Elgin & Molina Garza 1988). There are numerous other similar branches which are not illustrated in the figure, giving rise to a rich structure with many subsidiary bifurcations.

## 5. Conclusion

The partial differential equations (1) admit a trivial solution which loses stability in a Hopf bifurcation if $\tau < 1$ and $r_S > r_{SC} = \tau^2(1+\sigma)/\sigma(1-\tau)$. We have developed a hierarchy of low-order models to describe the behaviour of the resulting nonlinear oscillations. We began by substituting a truncated modal expansion into the partial differential equations. The simplest self-consistent nonlinear equations are then the fifth-order system (10), which provides an asymptotically valid description in the limit $|a| \ll \tau < 1$ (Veronis 1965). For $\tau \ll 1$ this system can be simplified to yield the third-order (Lorenz) system (12), which is valid provided $|a| \ll \tau \ll 1$. Both (10) and (12) are accurate in the neighbourhoods of Hopf and pitchfork bifurcations from the trivial solution. As well as these codimension-one bifurcations they both capture the bifurcation of codimension two that occurs for $r_S = r_{SC}$. Setting $r_S = r_{SC}(1+\mu)$, $r_T = 1+(r_{SC}/\tau)(1+\lambda)$, with $|\mu| \ll 1$ and $|\lambda| \ll 1$, we found that the pitchfork bifurcation is described by the normal form equation (20): then the branch of periodic solutions that emerges from the Hopf bifurcation at $\lambda = 0$ terminates in a heteroclinic bifurcation with an orbit connecting a symmetrical pair of saddle-points at $\lambda = \lambda_h$ $(0 < \lambda_h < \mu)$.

The third-order system (12) can also be recognized as simplified normal form equations for a multiple bifurcation at $\lambda = \mu = \varpi = 0$ with the symmetry

$$(a, d, e) \rightarrow (-a, -d, e)$$

(Spiegel 1987; Proctor & Weiss 1990). Hence we expect the system to be structurally stable in the neighbourhood of this bifurcation. By considering tall thin cells and proceeding to the limit $\varpi \rightarrow 0$ we can therefore extend the variety of behaviour captured accurately by this system. In particular, in this limit the system remains a valid approximation to the partial differential equations even when the heteroclinic orbit connects a pair of saddle-foci. For $\mu = O(\varpi)$ most of the oscillatory branch can be followed by averaging the equations but a different approach is needed at its end. The heteroclinic bifurcation occurs close to the pitchfork bifurcation, with $\lambda = \mu[1-O(\varpi)]$, and behaviour in this regime is governed by the canonical system (36), whose solutions exhibit chaotic behaviour. Thus chaos occurs where the system (36), and the systems (12) and (10), are rational approximations to the original partial differential equations, showing that chaotic oscillations can be found arbitrarily close to the onset of convection (Proctor & Weiss 1990). Theory predicts that as the bifurcation parameter $\lambda$ approaches $\lambda_h$ a multiplicity of periodic and chaotic states is encountered through the formation of bifurcation bubbles. In addition, subsidiary homoclinic and heteroclinic orbits form and these themselves give rise to similar bifurcation structures. Yet in spite of its complexity all this structure is organized by and linked to the primary heteroclinic orbit.

This route to the canonical system is not unique. Tall thin cells with $\varpi \ll 1$ are described by simplified partial differential equations (Proctor & Holyer 1986). In the neighbourhood of the codimension-two bifurcation these equations reduce to a fourth-order system which yields the canonical system (36) in the limit $\tau \ll 1$ (Proctor

& Weiss 1990). An alternative set of partial differential equations is obtained by proceeding first to the limit $\tau \ll 1$; in the neighbourhood of the codimension-two bifurcation these reduce to the third-order system (12) from which the canonical system was derived. In particular, therefore, our results are independent of the order in which the limits $\tau \to 0$, $\varpi \to 0$ are applied (Rucklidge 1992).

To be sure, we have only established that idealized thermosolutal convection leads to chaotic oscillations in a tiny corner of parameter space. Does the same mechanism generate chaos over a macroscopic parameter range when the aspect ratio $A$ is of order unity? Here we must rely on computation: numerical experiments with $A = 1.4$ ($\varpi \approx \frac{8}{3}$) do indeed show that chaotic behaviour persists over a significant range (Huppert & Moore 1976; Knobloch *et al.* 1986*b*; Moore *et al.* 1990*b*). Moreover, the Shil'nikov mechanism persists in the third-order and fifth-order systems with $\varpi = O(1)$ (Knobloch *et al.* 1986*b*). Of course these systems then possess chaotic solutions only in regimes where they are no longer valid approximations but there is strong circumstantial evidence that chaos in solutions of the partial differential equations is caused by the Shil'nikov mechanism too.

We have succeeded in clarifying the connection between the fifth-order system and the full equations. The relationship between low-order systems and thermosolutal convection differs significantly from that between the Lorenz system and Rayleigh–Bénard convection. Although the derivation of the Lorenz equations is equivalent to that of the fifth-order system, two-dimensional Rayleigh–Bénard convection does not display the same exotic behaviour as the Lorenz system (Moore & Weiss 1973; Curry *et al.* 1984). Here chaos appears at large values of $r_T$ because the truncated model cannot resolve narrow boundary layers in solutions of the partial differential equations (Marcus 1981). In contrast, the chaotic behaviour of interest here occurs at small amplitude, when such boundary layers are absent. Consequently, the fifth-order system preserves the essential bifurcation structure of the thermosolutal problem, including both the possibility of chaotic behaviour near the heteroclinic bifurcation and the subsequent saddle-node bifurcation at which the steady branch acquires stability. This is the simplest example of a macroscopic system where complicated behaviour is faithfully represented by a low-order model. Similar behaviour has been found near a codimension-three bifurcation for the more elaborate problem of rotating thermosolutal convection (Arnéodo, Coullet & Spiegel 1983; Arnéodo & Thual 1985) where solutions are described by a different third-order system related to the nonlinear oscillator invented by Moore & Spiegel (1966; Marzec & Spiegel 1980; see also Proctor & Weiss 1990).

Thermosolutal convection is typical of systems with competing stabilizing and destabilizing forces. Thus the same approach can be applied, for instance, to magnetoconvection, as outlined in the Appendix. Rucklidge (1992) discusses convection in the presence of imposed vertical or horizontal magnetic fields in the limits $\varpi \to 0$ and $\varpi \to 4$. Although we have only discussed two-dimensional models, we are confident that three-dimensional convection in a suitable container will display qualitatively similar behaviour. Nonlinear oscillations have been studied in experiments on thermohaline convection (Shirtcliffe 1969) though binary fluids are more suited to laboratory experiments (e.g. Rehberg & Ahlers 1986). Results, are, however, sensitive to imposed constraints: symmetry-breaking bifurcations occur when the point symmetry (3) is relaxed (Moore, Weiss & Wilkins 1990*a*, 1991) while travelling waves are preferred if the no-flux lateral boundary conditions (2*b*) are replaced by periodic boundary conditions (Knobloch *et al.* 1986*a*). Hence experiments in wide boxes typically show travelling waves rather than standing waves (periodic

oscillations). Unfortunately the treatment followed here cannot be extended to include the interaction between travelling waves and standing waves in the limit $\tau \downarrow 0$ as the corresponding system is degenerate.

We thank Alastair Rucklidge for his comments and for assistance in producing figures 3 and 5. We have also benefited from discussions with Paul Glendinning, Daniel Moore, Colin Sparrow and Edward Spiegel and with participants in the GFD Summer Program at Woods Hole Oceanographic Institution. SERC has generously provided a research grant, a Senior Fellowship (N.O.W.) and a Visiting Fellowship (E.K.); E.K. was also supported by NSF/DARPA under grant DMS-8814702.

## Appendix. Magnetoconvection

The partial differential equations governing two-dimensional Boussinesq convection in an imposed vertical magnetic field can be reduced to the truncated system

$$\dot{a} = \sigma[-a + r_T b - \zeta q d\{1 + (3-\varpi)e\}] + O(a^5\zeta^{-4}), \tag{A 1a}$$

$$\dot{b} = -b + a(1-c) + O(a^5), \tag{A 1b}$$

$$\dot{c} = \varpi(-c + ab) + O(a^4), \tag{A 1c}$$

$$\dot{d} = -\zeta d + a(1-e) + O(a^5\zeta^{-4}), \tag{A 1d}$$

$$\dot{e} = -(4-\varpi)\zeta e + \varpi ad + O(a^4\zeta^{-3}), \tag{A 1e}$$

where $q$ is a scaled Chandrasekhar number and $\zeta$ is the ratio of the magnetic to the thermal diffusivity (Knobloch, Weiss & Da Costa 1981; Proctor & Weiss 1982). This fifth-order system displays a greater variety of behaviour than the corresponding system (5) for thermosolutal convection, owing to the extra nonlinearity in (A 1*a*) introduced by the Lorentz force. We are interested in behaviour when $\zeta \ll 1$, so we set

$$r_T = 1 + \frac{\zeta(1+\sigma)}{\sigma}\hat{r}, \quad q = \frac{\zeta(1+\sigma)}{\sigma}\hat{q}, \quad \tilde{t} = \zeta t^*, \quad a = \zeta\tilde{a}, \quad b = \zeta\tilde{b}, \quad c = \zeta^2\tilde{c}. \tag{A 2}$$

In the limit as $\zeta \to 0$ and after tildes have been suppressed, (A 1) reduces to the third-order system

$$a' = \hat{r}a - \hat{q}d[1 + (3-\varpi)e], \tag{A 3a}$$

$$d' = -d + a(1-e), \tag{A 3b}$$

$$e' = -(4-\varpi)e + \varpi ad. \tag{A 3c}$$

This is a rational approximation to the full equation in the limit $|a| \ll 1$. Equations (A 3) again possess the symmetry $(a, d, e) \to (-a, -d, e)$ and the pitchfork bifurcation from the trivial solution occurs at $\hat{r} = \hat{q}$, preceded by a Hopf bifurcation at $\hat{r} = 1$ for $\hat{q} > 1$.

There is a codimension-two bifurcation with a double-zero eigenvalue at $\hat{r} = \hat{q} = 1$. To describe behaviour in the neighbourhood of this bifurcation we introduce a small parameter $\epsilon$ and set

$$\hat{r} = 1 + \epsilon^2\lambda, \quad \hat{q} = 1 + \epsilon^2\mu, \quad \tilde{t} = \epsilon t, \quad a = \epsilon\tilde{a}, \quad d = \epsilon\tilde{d}, \quad e = \epsilon^2\tilde{e}. \tag{A 4}$$

Suppressing tildes, we then obtain the normal form equation

$$a'' + (\mu - \lambda)a + \frac{\varpi(2-\varpi)}{(4-\varpi)}a^3 = \epsilon\left[\lambda - \frac{\varpi(\varpi^2 - 6\varpi + 12)}{(4-\varpi)^2}a^2\right]a' + O(\epsilon^2). \tag{A 5}$$

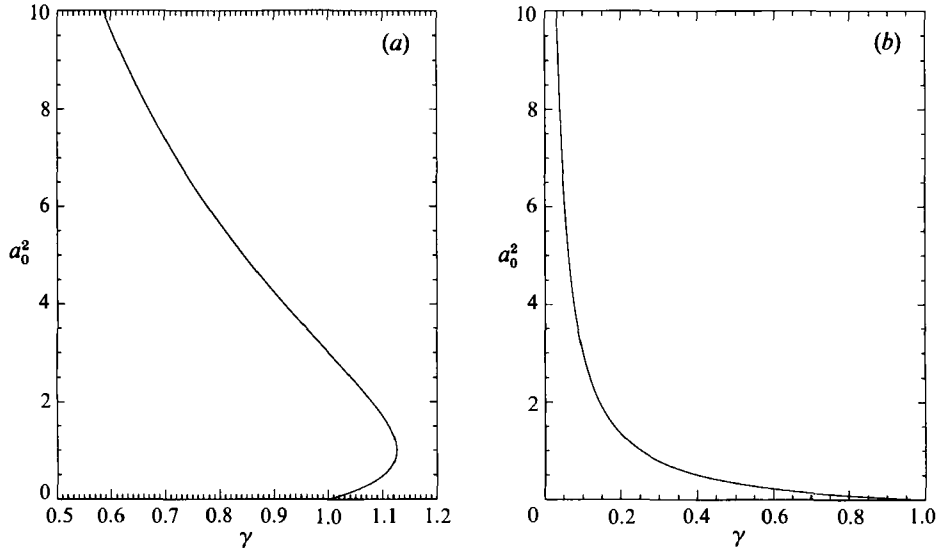


FIGURE 6. Steady nonlinear magnetoconvection: $a_0^2$ as a function of $\gamma = \hat{r}/\hat{q}$ for (*a*) $\varpi = 1$, with a turning point and (*b*) $\varpi = 3$. The Hopf bifurcation occurs at $\gamma = \hat{q}^{-1}$, for $\hat{q} > 1$.

The bifurcation structure changes when $\varpi = 2$. For $\varpi > 2$ there is subcritical steady convection and the oscillatory branch terminates in a heteroclinic bifurcation as for the thermosolutal problem. For $\varpi < 2$ there are steady solutions near the bifurcation only for $\lambda > \mu$ and the oscillatory branch eventually terminates in a Hopf bifurcation from the steady branch (Knobloch & Proctor 1981; Proctor & Weiss 1982; Arnol'd 1983; Guckenheimer & Holmes 1986).

The third-order system (A 3) possesses a steady solution with $a = a_0$ which depends only on the ratio $\gamma = \hat{r}/\hat{q}$. From (A 3),

$$\gamma = \frac{(4-\varpi)^2(1+\varpi a_0^2)}{[(4-\varpi)+\varpi a_0^2]^2}: \tag{A 6}$$

the steady branch emerges from the pitchfork bifurcation at $\gamma = 1$ with

$$\gamma = 1 + \frac{\varpi(2-\varpi)}{(4-\varpi)} a_0^2 + O(a_0^4), \tag{A 7}$$

cf. (A 5), and $\gamma \to 0$ as $a_0^2 \to \infty$. For $\varpi < 2$, $\gamma$ initially increases but there is a turning point, corresponding to a saddle-node bifurcation, at

$$a_0^2 = \frac{2-\varpi}{\varpi}, \quad \gamma = \frac{(4-\varpi)^2}{4(3-\varpi)}. \tag{A 8}$$

For $\varpi > 2$, $\gamma$ decreases monotonically with increasing $a_0^2$. Thus the steady branch has the forms shown in figure 6 and there is a degenerate bifurcation at $\varpi = 2$.

When $\varpi < 2$ there may be a secondary Hopf bifurcation from the steady branch. This first appears at the Bogdanov point, as a double-zero bifurcation when $\hat{q} = 1$. As $\hat{q}$ is increased the Hopf bifurcation creeps up the steady branch, until it reaches the saddle-node bifurcation when

$$\hat{q} \approx \left[\frac{2(3-\varpi)}{(4-\varpi)}\right]^2 \quad \text{and} \quad \hat{r} = 3-\varpi. \tag{A 9}$$

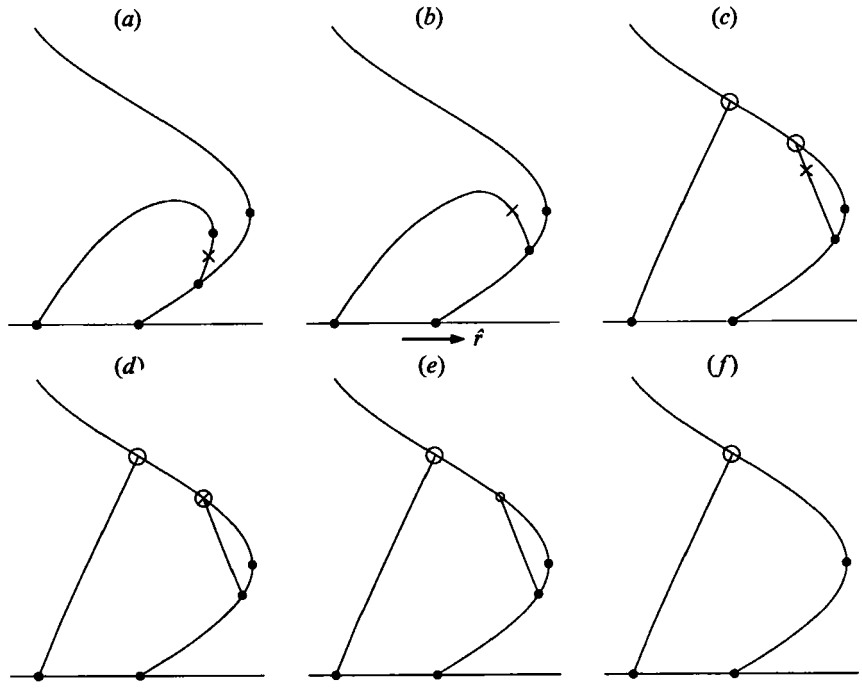


FIGURE 7. Global bifurcations in magnetoconvection for $\varpi = 1$. Sketches showing behaviour for (*a*) $\hat{q} = 1.2$, with a biclinic (gluing) bifurcation as described by the normal form equation (A 5); (*b*) $\hat{q} = 1.22$, with a supercritical Hopf bifurcation; (*c*) $\hat{q} = 1.25$, with a pair of heteroclinic bifurcations; (*d*) $\hat{q} = 1.27$, where the biclinic bifurcation coincides with a heteroclinic bifurcation; (*e*) $\hat{q} = 1.3$, with a homoclinic and a heteroclinic bifurcation; (*f*) $\hat{q} = 2$, with a single oscillatory branch terminating in a heteroclinic bifurcation. Small open circles, large open circles and crosses denote homoclinic, heteroclinic and biclinic bifurcations respectively; local bifurcations are indicated by filled circles.

Here there is again a double-zero eigenvalue; behaviour in the neighbourhood of this codimension-two bifurcation is described by the normal form equations for coincident Hopf and saddle-node bifurcations (Arnol'd 1983; Guckenheimer & Holmes 1986).

A full description of the evolution of the oscillatory branch involves a variety of global bifurcations. We have carried out a numerical investigation of behaviour with $\varpi = 1$ and the results are summarized in figure 7. For $\hat{q}$ sufficiently close to unity solutions follow the pattern predicted by the normal form equation (A 5) (Knobloch & Proctor 1981; Proctor & Weiss 1982). At $\hat{q} = 1.2$, for example, there is an oscillatory branch with stable symmetric limit cycles enclosing the origin for $1 < r < 1.303$; this branch loses stability in a saddle-node bifurcation and the unstable oscillations undergo a biclinic (gluing) bifurcation as indicated in figure 7(*a*) (cf. Nagata, Proctor & Weiss 1990). This is followed by a pair of unstable asymmetric limit cycles, which collapse on to the steady branch in a subcritical Hopf bifurcation at $\hat{r} = 1.297$. By $\hat{q} = 1.22$ behaviour is affected by the upper portion of the steady branch and the entire oscillatory branch, including the asymmetric orbits, is stable up to a supercritical Hopf bifurcation at $\hat{r} = 1.33$, as sketched in figure 7(*b*). At $\hat{q} = 1.23$ a heteroclinic bifurcation appears on the oscillatory branch. Thereafter the branch splits into two segments, each of which ends in a heteroclinic bifurcation, as shown in figure 7(*c*) for $\hat{q} = 1.25$. Here the branch emerging from the initial Hopf bifurcation at $\hat{r} = 1$ terminates in a heteroclinic bifurcation at $\hat{r} = 1.338$; the branch

of asymmetric oscillations that emerges from the secondary Hopf bifurcation first undergoes a biclinic bifurcation leading to symmetric oscillations and the segment terminates in a heteroclinic bifurcation at $\hat{r} = 1.364$. (Note that the order of these transitions may depend on the choice of $\varpi$.)

The two global bifurcations on the second segment approach each other as $\hat{q}$ is increased until there is a codimension-two point at $\hat{q} = 1.27$, $\hat{r} = 1.3888$, with simultaneous biclinic and heteroclinic bifurcations, as sketched in figure 7(*d*). From then on there are only asymmetric oscillations on the second segment, which terminates in a homoclinic bifurcation, as shown in figure 7(*e*) for $\hat{q} = 1.3$. This segment shrinks as $\hat{q}$ is further increased and finally disappears at the codimension-two point when the Hopf and saddle-node bifurcations coincide. From (A 9) this occurs when $\hat{q} = 1.7778$, with $\hat{r} = 2$. Behaviour near this point is consistent with the appropriate normal form equations.

For $\hat{q}$ greater than this value, only the first segment remains, as sketched in figure 7(*f*) for $\hat{q} = 2$. Subsequent behaviour resembles that already found for thermosolutal convection. As $\hat{q}$ increases, the heteroclinic bifurcation rises up the steady branch and the fixed points change from saddles to saddle-foci. A bubble structure develops, with symmetry-breaking and period-doubling bifurcations at $\hat{q} = 4$. Finally, the Shil'nikov mechanism leads to chaos when $\hat{q} = 5$.

The most significant feature of these results is the appearance of a heteroclinic bifurcation which splits the oscillatory branch into two separate segments. Although the third-order system (A 3) is no longer a valid asymptotic approximation to the partial differential equations when this happens, we still expect the behaviour summarized in figure 7 to occur both in the fifth-order system (A 1) and in the partial differential equations themselves. The bifurcation structure is thus characteristic of the parameter regime in which the oscillatory instability is supercritical and the steady branch has the form shown in figure 7. This structure could be described by unfolding the degenerate bifurcation at $\varpi = 2$ (cf. Dangelmayr, Armbruster & Neveling 1985; Knobloch & Proctor 1988). It is also possible to simplify (A 3) in the neighbourhood of the triple bifurcation at $\varpi = 4$ but this limit is physically unrealistic, since rolls with smaller aspect ratios would become unstable first. Rucklidge (1992) finds more interesting behaviour for $\varpi \ll 1$, where the Hopf bifurcation at $\mu = \lambda$ is subcritical, and has also investigated the analogous problem with a horizontal field.

## REFERENCES


Arnéodo, A., Coullet, P. H. & Spiegel, E. A. 1985 The dynamics of triple convection. *Geophys. Astrophys. Fluid Dyn.* **31**, 1–48.

Arnéodo, A. & Thual, O. 1985 Direct numerical simulations of a triple convection problem versus normal form predictions. *Phys. Lett.* **109A**, 367–373.

Arnol'd, V. I. 1983 *Geometrical Methods in the Theory of Ordinary Differential Equations*. Springer.

Bernoff, A. J. 1986 Transitions from order in convection. Ph.D. thesis, University of Cambridge.

Coullet, P. H. & Spiegel, E. A. 1983 Amplitude equations for systems with competing instabilities. *SIAM J. Appl. Maths.* **43**, 776–821.

Curry, J. H., Herring, J. R., Loncaric, J. & Orszag, S. A. 1984 Order and disorder in two- and three-dimensional Bénard convection. *J. Fluid Mech.* **147**, 1–38.

Da Costa, L. N., Knobloch, E. & Weiss, N. O. 1981 Oscillations in double-diffusive convection. *J. Fluid Mech.* **109**, 25–43.

Dangelmayr, G., Armbruster, D. & Neveling, M. 1985 A codimension three bifurcation for the laser with saturable absorber. *Z. Phys.* B **59**, 365–370.

Elgin, J. N. & Molina Garza, J. B. 1988 On the travelling wave solutions of the Maxwell–Bloch

equations. In *Structure, Coherence and Chaos in Dynamical Systems* (ed. P. Christiansen & R. D. Parmentier), pp. 553–562. Manchester University Press.

GLENDINNING, P. A. & SPARROW, C. T. 1984 Local and global behaviour near homoclinic orbits. *J. Statist. Phys.* **35**, 645–696.

GUCKENHEIMER, J. & HOLMES, P. 1986 *Nonlinear Oscillations, Dynamical Systems and Bifurcations of Vector Fields* (2nd printing). Springer.

HUPPERT, H. E. & MOORE, D. R. 1976 Nonlinear double-diffusive convection. *J. Fluid Mech.* **78**, 821–854.

KNOBLOCH, E., DEANE, A. E., TOOMRE, J. & MOORE, D. R. 1986*a* Doubly diffusive waves. *Contemp. Maths* **56**, 203–216.

KNOBLOCH, E., MOORE, D. R., TOOMRE, J. & WEISS, N. O. 1986*b* Transitions to chaos in two-dimensional double-diffusive convection. *J. Fluid Mech.* **166**, 409–448.

KNOBLOCH, E. & PROCTOR, M. R. E. 1981 Nonlinear periodic convection in double-diffusive systems. *J. Fluid Mech.* **108**, 291–316.

KNOBLOCH, E. & PROCTOR, M. R. E. 1988 The double Hopf bifurcation with 2:1 resonance. *Proc. R. Soc. Lond.* A **415**, 61–90.

KNOBLOCH, E. & WEISS, N. O. 1983 Bifurcations in a model of magnetoconvection. *Physica* **9D**, 379–407.

KNOBLOCH, E., WEISS, N. O. & DA COSTA, L. N. 1981 Oscillatory and steady convection in a magnetic field. *J. Fluid Mech.* **113**, 153–186.

LORENZ, E. N. 1963 Deterministic nonperiodic flow. *J. Atmos. Sci.* **20**, 130–141.

MARCUS, P. S. 1981 Effects of truncation in modal representations of thermal convection. *J. Fluid Mech.* **103**, 241–255.

MARZEC, C. J. & SPIEGEL, E. A. 1980 Ordinary differential equations with strange attractors. *SIAM J. Appl. Maths* **38**, 403–421.

MOORE, D. R. & WEISS, N. O. 1973 Two-dimensional Rayleigh–Bénard convection. *J. Fluid Mech.* **58**, 289–312.

MOORE, D. R. & WEISS, N. O. 1990 Dynamics of double convection. *Phil. Trans. R. Soc. Lond.* A **332**, 121–134.

MOORE, D. R., WEISS, N. O. & WILKINS, J. M. 1990*a* Symmetry-breaking in thermosolutal convection. *Phys. Lett.* A **147**, 209–214.

MOORE, D. R., WEISS, N. O. & WILKINS, J. M. 1990*b* The reliability of numerical experiments: transitions to chaos in thermosolutal convection. *Nonlinearity* **3**, 997–1014.

MOORE, D. R., WEISS, N. O. & WILKINS, J. M. 1991 Asymmetric oscillations in thermosolutal convection. *J. Fluid Mech.* **233**, 561–585.

MOORE, D. W. & SPIEGEL, E. A. 1966 A thermally excited nonlinear oscillator. *Astrophys. J.* **143**, 871–887.

NAGATA, M., PROCTOR, M. R. E. & WEISS, N. O. 1990 Transitions to asymmetry in magnetoconvection. *Geophys. Astrophys. Fluid Dyn.* **51**, 211–241.

PROCTOR, M. R. E. 1981 Steady subcritical thermohaline convection. *J. Fluid Mech.* **105**, 507–521.

PROCTOR, M. R. E. & HOLYER, J. Y. 1986 Planform selection in salt fingers. *J. Fluid Mech.* **168**, 241–253.

PROCTOR, M. R. E. & WEISS, N. O. 1982 Magnetoconvection. *Rep. Prog. Phys.* **45**, 1317–1379.

PROCTOR, M. R. E. & WEISS, N. O. 1990 Normal forms and chaos in thermosolutal convection. *Nonlinearity* **3**, 619–637.

REHBERG, I. & AHLERS, G. 1986 Codimension two bifurcation in a convection experiment. *Contemp. Maths* **56**, 277–282.

RUCKLIDGE, A. M. 1992 Chaos in models of double convection. *J. Fluid Mech.* **237**, 209–229.

SHIL'NIKOV, L. P. 1965 A case of the existence of a countable number of periodic motions. *Sov. Math. Dokl* **6**, 163–166.

SHIRTCLIFFE, T. G. L. 1969 An experimental investigation of thermosolutal convection at marginal stability. *J. Fluid Mech.* **35**, 671–688.

SPARROW, C. T. 1982 *The Lorenz Equations: Bifurcations, Chaos and Strange Attractors*. Springer.

SPIEGEL, E. A. 1987 Chaos: a mixed metaphor for turbulence. *Proc. R. Soc. Lond.* A **413**, 87–95.

TRESSER, C. 1984 About some theorems by L. P. Shil'nikov. *Ann. Inst. H. Poincaré* **40**, 440–461.

VERONIS, G. 1965 On finite amplitude instability in thermohaline convection. *J. Mar. Res.* **23**, 1–17.

WEISS, N. O. 1987 Dynamics of convection. *Prog. R. Soc. Lond.* A **413**, 71–85.

WIGGINS, S. 1988 *Global Bifurcations and Chaos*. Springer.